J. Am. Soc. Mass Spectrom. (2017)
DOI: 10.1007/s13361-017-1787-8

FOCUS: 29th SANIBEL CONFERENCE, PEPTIDOMICS: BRIDGING THE GAP BETWEEN PROTEOMICS AND METABOLOMICS BY MS: RESEARCH ARTICLE

Towards Discovery and Targeted Peptide Biomarker Detection Using nanoESI-TIMS-TOF MS

Alyssa Garabedian,[1] Paolo Benigni,[1] Cesar E. Ramirez,[1] Erin S. Baker,[2] Tao Liu,[2] Richard D. Smith,[2] Francisco Fernandez-Lima[1,3]

[1]Department of Chemistry and Biochemistry, Florida International University, Miami, FL 33199, USA
[2]Biological Sciences Division and Environmental Molecular Sciences Laboratory, Pacific Northwest National Laboratory, Richland, WA 99352, USA
[3]Biomolecular Sciences Institute, Florida International University, Miami, FL 33199, USA

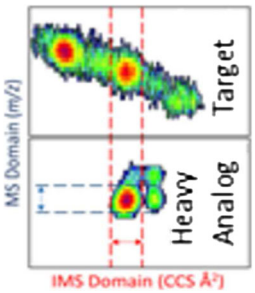

Abstract. In the present work, the potential of trapped ion mobility spectrometry coupled to TOF mass spectrometry (TIMS-TOF MS) for discovery and targeted monitoring of peptide biomarkers from human-in-mouse xenograft tumor tissue was evaluated. In particular, a TIMS-MS workflow was developed for the detection and quantification of peptide biomarkers using internal heavy analogs, taking advantage of the high mobility resolution (R = 150–250) prior to mass analysis. Five peptide biomarkers were separated, identified, and quantified using offline nanoESI-TIMS-CID-TOF MS; the results were in good agreement with measurements using a traditional LC-ESI-MS/MS proteomics workflow. The TIMS-TOF MS analysis permitted peptide biomarker detection based on accurate mobility, mass measurements, and high sequence coverage for concentrations in the 10–200 nM range, while simultaneously achieving discovery measurements of not initially targeted peptides as markers from the same proteins and, eventually, other proteins.

Keywords: Discovery and targeted monitoring, Trapped ion mobility spectrometry, Mass, Spectrometry, Biomarker detection, Quantitative proteomics

Received: 30 May 2017/Revised: 29 July 2017/Accepted: 10 August 2017

Introduction

The level of chemical complexity during proteomic analysis and the large dynamic range of commonly studied and potential biomarkers represent an analytical challenge that requires the further development of high throughput, orthogonal, reproducible, and robust analytical platforms. Nowadays, mass spectrometry-based analysis offers an unparalleled, non-targeted, analysis tool for dissecting complex protein samples at the molecular level; however, prior to mass spectrometry analysis, pre-separation techniques, such as high performance liquid chromatography (HPLC) and nano-liquid chromatography (nanoLC) are often required to enhance the peak capacity of the analysis. In addition, these pre-separation methods can provide advantages by reducing problems associated with ion suppression during competitive ionization of complex samples, a phenomenon that is more typically observed during biomarker detection across a large dynamic range [1, 2]. However, traditional LC-based protocols require long separation times in order to separate the compounds of interest and high solvent consumption, which for large scale profiling represents a major obstacle in analysis due to added cost [3–5]. In addition, these techniques still suffer from poor separation of isobaric species, which significantly challenges protein sequencing and identification using bottom-up approaches. These challenges become major hindrances for the analysis of a complex biological system such as cancer proteomic samples, which typically contain a myriad of molecular species. In addition, large-scale

Electronic supplementary material The online version of this article (https://doi.org/10.1007/s13361-017-1787-8) contains supplementary material, which is available to authorized users.

Correspondence to: Francisco Fernandez–Lima; *e-mail:* fernandf@fiu.edu

Published online: 09 September 2017

profiling in bottom-up proteomics is often limited by the sensitivity of the current mass spectrometry instruments to isolate and detect parent and fragment ions during tandem MS analysis of complex mixtures [6]. For example, current bottom-up proteomic strategies require the chemical treatment of samples (i.e., trituration, protein extraction, enzymatic digest) prior to analysis, which result in highly complex mixtures that then require further separation and preparation prior to MS analysis [7].

An alternative or complementary approach is the use of gas-phase, post-ionization separations such as ion mobility spectrometry coupled to mass spectrometry (IMS-MS), which promises further gains in the speed, sensitivity, and selectivity for the analysis of complex biological mixtures [8, 9]. Specifically, the added mobility dimension of separation yields an increase in peak coverage [6, 10–12], a factor that has often inhibited the analysis of complex mixtures with MS-only detection. The IMS-MS coupling readily enhances peptide/protein coverage and identification by allowing more ions, specifically isomers, to be resolved while simultaneously reducing chemical noise [13, 14]. Previous studies have illustrated the advantages of IMS-MS in terms of profiling mixtures [8, 15–19], making it one of the most powerful platforms for identification and characterization of proteins and peptides in biological samples. Our group has been working on the development of alternative, time-independent IMS approaches based on trapped ion mobility spectrometry coupled to MS (TIMS-TOF MS and TIMS-FT-ICR MS) for the study and manipulation of gas-phase molecular ions [10, 20–33]. Briefly, the concept behind TIMS is the use of an electric field to hold ions stationary against a moving gas, so that the drift force is compensated by the electric field and ion packets are separated based on their respective ion mobilities [20, 21, 27]. This concept follows the idea of a parallel flow ion mobility analyzer [34], with the main difference that ions are also confined radially using a quadrupolar field to guarantee higher ion transmission and sensitivity [20, 21]. Since the introduction of TIMS-MS in 2011 [20, 21], our group [10, 22–33, 35] and others [8, 36–44] have shown the potential of TIMS-MS for fast, gas-phase separation and for molecular structural elucidation. In particular, we have demonstrated the advantages of TIMS over traditional IMS analyzers for fast screening [22] and targeted [10, 35] analysis of molecular ions from complex chemical mixtures, the study of isomerization kinetics of small molecules [23, 24], peptides [25], DNA [33], proteins [28, 29], DNA–protein complexes, and protein–protein complexes in their native and denatured states [32]. In a more recent report, we showed the isomer separation of polybrominated diphenyl ether metabolites using nanoESI-TIMS-TOF MS with mobility resolutions of up to 400 (the highest reported mobility resolution for singly charged species) [30].

Herein, we present for the first time a nanoESI-TIMS-CID-TOF MS workflow, developed for fast, gas-phase ion separation and accumulation, with efforts focused on targeted quantitative analysis and discovery measurements of breast cancer markers. The ability of TIMS-CID-TOF MS to separate and sequence isobaric peptides in a complex mixture is illustrated. We address typical challenges and targeted discovery monitoring strategies using isotopically labeled internal standards for effective peptide identification and sequencing. Although LC-TIMS-MS separations were recently shown in the case of peptide markers [8], the presented workflow targets offline separations in order to shorten the MS analysis time while tailoring the TIMS analysis for high mobility separation and sensitivity.

Experimental

Tumor Protein Extraction and Tryptic Digestion

A patient-derived mouse xenograft model of luminal B human breast cancer – Washington University Human-in-Mouse (WHIM16) – was used for all the studies [45]. The WHIM16 xenograft tumor pieces were transferred into precooled Covaris Tissue-Tube 1 Extra (TT01xt) bags (Covaris no. 520007) and processed in a Covaris CP02 Cryoprep device using an impact setting of 3 (all tumor tissue wet weights were less than 100 mg). The tissue powder was then transferred into precooled cryovials (Corning no. 430487). All procedures were carried out on dry ice and liquid nitrogen to maintain tissue in a powdered, frozen state. Approximately 50 mg of WHIM16 tumor tissue was homogenized in 600 µL of lysis buffer (8 M urea, 100 mM NH_4HCO_3, pH 7.8, 0.1% NP-40, 0.5% sodium deoxycholate, 10 mM NaF, phosphatase inhibitor cocktails 2 and 3, 20 µM PUGNAc). Protein concentrations of tissue lysates were determined by BCA assay (Pierce). Proteins were reduced with 5 mM dithiothreitol for 1 h at 37 °C, and subsequently alkylated with 10 mM iodoacetamide for 1 h at room temperature in the dark. Samples were diluted 1:2 with Nanopure water, 1 mM $CaCl_2$ and digested with sequencing grade modified trypsin (Promega, V5113) at 1:50 enzyme-to-substrate ratio. After 4 h of digestion at 37 °C, samples were diluted 1:4 with the same buffers and another aliquot of the same amount of trypsin was added to the samples and further incubated at room temperature overnight (~16 h). The digested samples were then acidified with 10% trifluoroacetic acid to ~pH 3. Tryptic peptides were desalted on strong cation exchange (SCX) SPE (SUPELCO, Discovery-SCX, 52685-U) and reversed-phase C18 SPE columns (SUPELCO Discovery, 52601-U) and dried using Speed-Vac.

Tryptic Peptide Fractionation

The tryptic peptide sample was separated on a Waters reverse phase XBridge C18 column (250 × 4.6 mm, 5-µm and protected by a 4.6 mm × 20 mm guard column) using an Agilent 1200 HPLC System. After sample loading, the column was washed for 35 min with 10 mM triethylammonium bicarbonate, pH 7.5 (solvent A), before applying a 102-min LC gradient in combination with 10 mM triethylammonium bicarbonate, pH 7.5, 90% acetonitrile (solvent B). The LC gradient started with a linear increase to 10% B in 6 min, then to 30% B

in 86 min, 42.5% B in 10 min, 55% B in 5 min, and 100% solvent B in another 5 min. The flow rate was 0.5 mL/min. A total of 96 fractions were collected into a 96 well plate throughout the LC gradient. These fractions were concatenated into 48 fractions by combining two fractions that are 48 fractions apart (i.e., combining fractions #1 and #49; #2 and #50; and so on) [46]. The concatenated fractions were dried in a Speed-Vac and stored at −80 °C. Fractions of various volumes were prepared at PNNL based upon BCA analyses to have total peptide concentrations of 0.5 μg/μL and shipped for analysis at FIU. The fractions of interest were selected a priori based on LC-MS/MS analyses conducted at PNNL (to be reported separately) with known presence of the target peptides of interest in this study (see Table 1). Heavy standards of the target peptides were purchased from ThermoFisher and used as received. The last residue of the sequence (Arg or Lys) was modified with ^{13}C6 and ^{15}N4 or ^{13}C6 and ^{15}N2, respectively. Light (non-isotopically labeled) standards of the target peptides were also purchased from GenScript and used without further purification. All samples were diluted with Optima grade 0.1% formic acid in water.

Trapped Ion Mobility Spectrometry-Mass Spectrometry Analysis

Individual fractions, each spiked with the corresponding internal heavy peptide standard, were analyzed by directly infusing the sample via nanoESI into the TIMS-MS spectrometer. A detailed overview of the TIMS analyzer and its operation can be found elsewhere [20, 21, 27]. The nitrogen bath gas flow is defined by the pressure difference between entrance funnel P_1 = 1.8–2.6 mbar and the exit funnel P_2 = 0.6–1.0 mbar at ca. 300 K. The TIMS analyzer is comprised of three regions: an entrance funnel, analyzer tunnel (46 mm axial length), and exit funnel. A 880 kHz and 200 V_{pp} rf potential was applied to each section, creating a dipolar field in the funnel regions and a quadrupolar field inside the tunnel. In TIMS operation, multiple ion species are trapped simultaneously at different E values resulting from a voltage gradient applied across the TIMS tunnel. After thermalization, species are eluted from the TIMS cell by decreasing the electric field in stepwise decrements (referred to as the "ramp") and can be described by a characteristic voltage (i.e., $V_{elution} - V_{out}$). Eluted ions are then mass analyzed and detected by a maXis impact Q-TOF MS (Bruker Daltonics Inc, Billerica, MA, USA).

In a TIMS device, the total analysis time can be described as:

$$\text{total IMS time} = t_{trap} + \left(V_{elution}/V_{ramp}\right) * t_{ramp} + TOF \quad (1)$$

$$= t_o + \left(V_{elut}/V_{ramp}\right) * t_{ramp}$$

where, t_{trap} is the thermalization/trapping time, TOF is the time after the mobility separation, and V_{ramp} and t_{ramp} are the voltage range and time required to vary the electric field, respectively. The elution voltage was experimentally determined by varying the ramp time (t_{ramp} = 100, 200, 300, 400, and 500 ms) for a constant ramp voltage. This procedure also determines the time ions spend outside the separation region t_o (e.g., ion trapping and time-of-flight). The TIMS cell was operated using a fill/trap/ramp/wait sequence of 10/10/50–500/50 ms. The TOF analyzer was operated at 10 kHz (*m/z* 100–3500). The data was summed over 100 analysis cycles yielding an analysis time of ~50 s for the largest trapping times (t_{ramp} = 500 ms). Mobility calibration was performed using the Tuning Mix calibration standard (G24221A; Agilent Technologies, Santa Clara, CA, USA) in positive ion mode (e.g., *m/z* 322, K_0 = 1.376 $cm^2\ V^{-1}\ s^{-1}$ and *m/z* 622, K_0 = 1.013 $cm^2\ V^{-1}\ s^{-1}$) [27]. The TIMS operation was controlled using in-house software, written in National Instruments Lab VIEW, and synchronized with the maXis Impact Q-TOF acquisition program [20]. A custom-built source using pulled capillary nanoESI emitters was utilized for all the experiments. Quartz glass capillaries (o.d.: 1.0 mm and i.d.: 0.70 mm) were pulled utilizing a P-2000 micropipette laser puller (Sutter Instruments, Novato, CA, USA) and loaded with 10 μL aliquot of the 20× diluted sample solution. A typical nanoESI source voltage of +600–1200 V was applied between the pulled capillary tips and the TIMS-MS instrument inlet. Ions were introduced via a stainless steel inlet capillary (1/16 × 0.020″, IDEX Health Science,

Table 1. Peptide Sequence, *m/z* of Light and Heavy Peptides, Ion-Neutral Collision Cross-Section (CCS), and Total In-Fraction Peptide Concentration of the Five Targeted Biomarkers

Peptide	*m/z*	CCS_{N2} (Å^2)	Concentration (nM)
DFTPAELR	948.483 $[M+H]^+$	298	182±7.0
DFTPAEL**R**	958.486 $[M+H]^+$	298	
TTILQSTGK	948.521 $[M+H]^+$	295	21 ± 5.0
TTILQSTG**K**	956.555 $[M+H]^+$	295	(19 ± 3.0*)
DVVICPDASLEDAKK	801.904 $[M+2H]^+$	430	18 ± 5.0
DVVICPDASLEDAK**K**	834.422 $[M+2H]^{+2}$	436	(19.0 ± 3.0*)
LSASTASELSPK	595.815 $[M+2H]^{+2}$	380	17±4.8
LSASTASELSP**K**	599.824 $[M+2H]^{+2}$	380	
VFDKDGNGYISAAELR	877.925 $[M+2H]^{+2}$	452	16 ± 4.5
VFDKDGNGYISAAEL**R**	882.944 $[M+2H]^{+2}$	452	(15± 3.0*)

LC-ESI-MS/MS concentrations using the 535.2 ➔187.0 Da (DVVICPDASLEDAKK), 585.7 ➔ 201.1 Da (VFDKDGNGYISAAELR), and 474.9 ➔ 130.1 Da (TTILQSTGK) channels are denoted with an asterisk (*)

Oak Harbor, WA, USA) held at room temperature into the TIMS cell.

Reduced mobility values (K_0) were correlated with Collisional cross section (Ω) using the equation:

$$\Omega = \frac{(18\pi)^{1/2}}{16}\frac{z}{(k_B T)^{1/2}}\left[\frac{1}{m_i}+\frac{1}{m_b}\right]^{1/2}\frac{1}{K_0}\frac{1}{N^*} \quad (2)$$

where z is the charge of the ion, k_B is the Boltzmann constant, N^* is the number density, and m_i and m_b refer to the masses of the ion and bath gas, respectively [47]. All IMS resolving power ($R_{IMS} = \Omega/\Delta\Omega$) and mass resolution ($R_{MS} = m/\Delta m$) values were determined from Gaussian peak fits using OriginPro (version 8.0).

LC-ESI-MS/MS Analysis

Confirmation studies using tandem mass spectrometry were performed by a QTRAP 5500 triple-quadrupole mass spectrometer (AB SCIEX, Concord, ON, Canada) equipped with a Turbo V ion source (ESI) operated in the positive mode. Solutions of peptides and heavy analogs (5.0 µM) in 50% acetonitrile, 0.1% formic acid in water were directly infused (10 µL/min) into the TurboV ion source. Once suitable species (usually $[M+2H]^{+2}$) were detected in manual tuning mode, automatic optimization was performed of the collision energy (CE), declustering potential (DP), and collision cell exit potential (CXP) to obtain best parameters for MS/MS via collision-induced dissociation (CID). A multiple reaction monitoring (MRM) detection method was thus developed for each peptide and heavy analog, using the two most intense transitions observed for quantitative and confirmation purposes. HPLC separations (40 µL injections) used a reverse phase column (Dionex Acclaim 120 C18 Column, 250 × 2.1 mm, 5 µm) and a Shimadzu Prominence LC-20AD ultra-fast liquid chromatograph. Mobile phase gradient was performed between 0.1% formic acid dissolved in water (mobile phase A) and 0.1% formic acid dissolved in acetonitrile (mobile phase B), all purchased commercially and of Optima LC-MS grade. The auto sampler was kept at 4 °C. Analysis was performed at 35 °C with a flow rate of 0.80 mL/min, according to the following 11.0 min program: hold 10% B for 0.25 min; ramp to 65% B in 4.5 min; ramp to 98% in 0.1 min; hold for 1.65 min; return to 10% B in 0.5 min; hold for 4 min until end.

Results and Discussion

Commonly used peptide biomarkers during detection of protein DJ-1 [48], calmodulin [49], parafibromin [50, 51], MAP7 domain-containing protein 1 [52–54], and membrane-associated progesterone receptor component 1 [55, 56] (sequences: DVVICPDASLEDAKK, VFDKDGNGYISAAELR, TTILQSTGK, LSASTASELSPK, DFTPAELR, respectively) were used in this study (see Table 1). The selection of the targeted peptides was guided towards covering a diverse protein abundance range based on previous analyses of the patient-derived breast cancer mouse xenograft tissue sample (WHIM16) using LC-QQQ by the Clinical Proteomic Tumor Analysis Consortium (CPTAC) [57]. Single peptide standards and their respective heavy versions were analyzed using TIMS-MS in order to determine the charge state distribution (CSD) and collision cross section (CCS) when sprayed from the same starting solvent

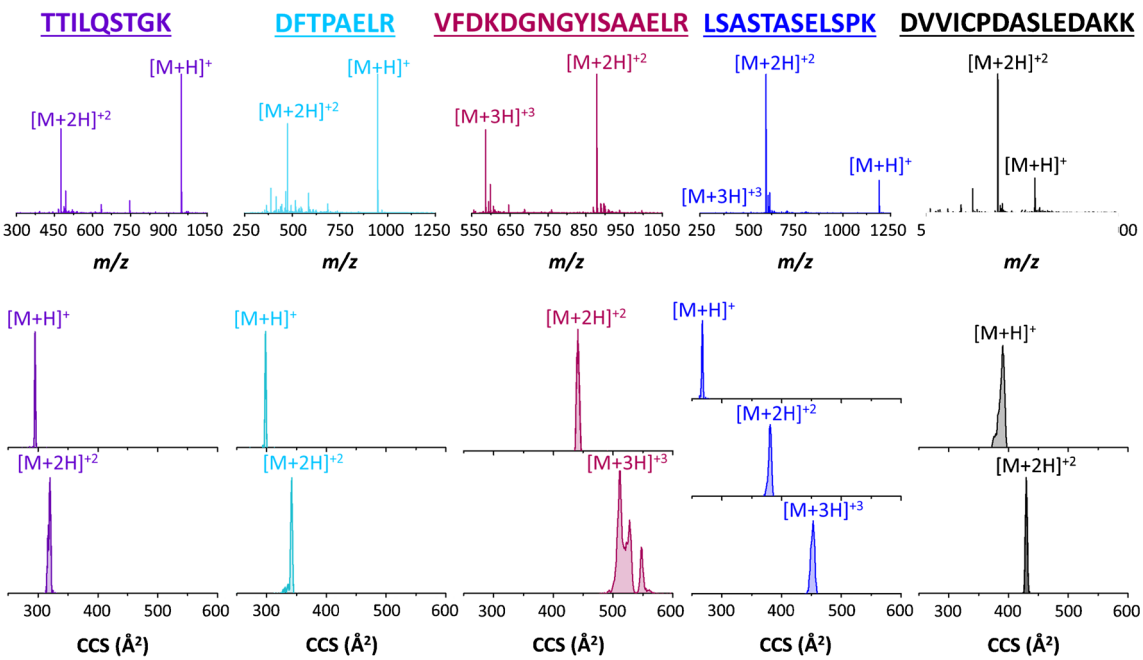

Figure 1. Typical mass spectra and IMS projection plots of the five targeted peptide of interest. Notice the high mobility resolution obtained using nanoESI-TIMS-TOF MS for single and double charged molecular ions

conditions as those of the WHIM16 tryptic digested fractions. Peptides DFTPAELR and TTILQSTGK showed similar CSDs with the $[M+H]^+$ producing the most abundant signal, whereas LSASTASELSPK, VFDKDGNGYISAAELR, and DVVICPDASLEDAKK showed larger abundance for the $[M+2H]^{+2}$ charge state (Figure 1). In addition to targeting *m/z* peaks, based on their abundance as a function of the charge state, a second criterion utilized was the simplicity of the CCS profiles for the $[M+H]^+$ and $[M+2H]^{+2}$ charge states in order to avoid potential interferences. A typical mobility resolving power of R > 200 was obtained for the $[M+H]^+$ and $[M+2H]^{+2}$ charge states, and CCS values correlate well with previously identified peptide mobility trend lines observed during IMS-MS analysis [58]. Comparison of the IMS profiles of the targeted peptides and the heavy analogs present the same distribution and CCS values (Table 1); moreover, an exception to this rule was observed for CAM modified heavy analogs customized to prevent disulfide association. For the latter, the confirmation and quantification was made based on the targeted and heavy analog *m/z* and CCS values.

The power of TIMS-MS for peptide characterization was further examined by sequencing two of the targeted peptides possessing the same nominal mass (e.g., *m/z* 948.479 and *m/z* 948.536 for DFTPAELR and TTILQSTGK, respectively). While traditional proteomics analysis is based on peptide identification using MS/MS strategies, for TIMS-CID-TOF MS the *m/z* and CCS characterization of the parent ion can be complemented with CID without the need for *m/z* preselection if separation in the CCS domain is achieved (Figure 2). Inspection of the experimental 2D IMS-MS contour plots of the isobaric peptide mixture shows the fragment ions of DFTPAELR and TTILQSTGK peptides falling directly in line with the mobilities of their respective parent ion (Figure 2a). The incorporation of IMS prior to CID holds multiple advantages for molecular identification since direct correlation of fragment ions with precursor ions can be performed in the 2D-IMS-MS domain [59–65]. Analysis using TIMS provided baseline separation of the targeted peptides, where a minimum resolving power of R_{IMS} ~100–150 (i.e., CCS of 295 and 298 $Å^2$) is required for near baseline separation (Figure 2b). Closer inspection of the product ions (mostly b and y type fragments and some internal fragments) permitted the verification of the peptide sequences (Figure 2c). The advantage of this approach compared with traditional LC-MS/MS proteomics is that the CCS values (or profiles) of each parent and corresponding fragments are common parameters to the IMS separation and can be used as additional identification confirmation. That is, the precursor and product ions will share the same CCS, while characteristic LC elution times may depend on several experimental conditions and may not be as reproducible, or specific, to a given peptide. However, because the CCS is a property of the peptide parent ion, the possibility to uniquely trap the mobility range of interest in a TIMS analyzer significantly enhances the multiple reaction monitoring capabilities of the TIMS-MS analyzer by ultimately reducing chemical noise and increasing the TIMS selectivity of the parent and fragment ions.

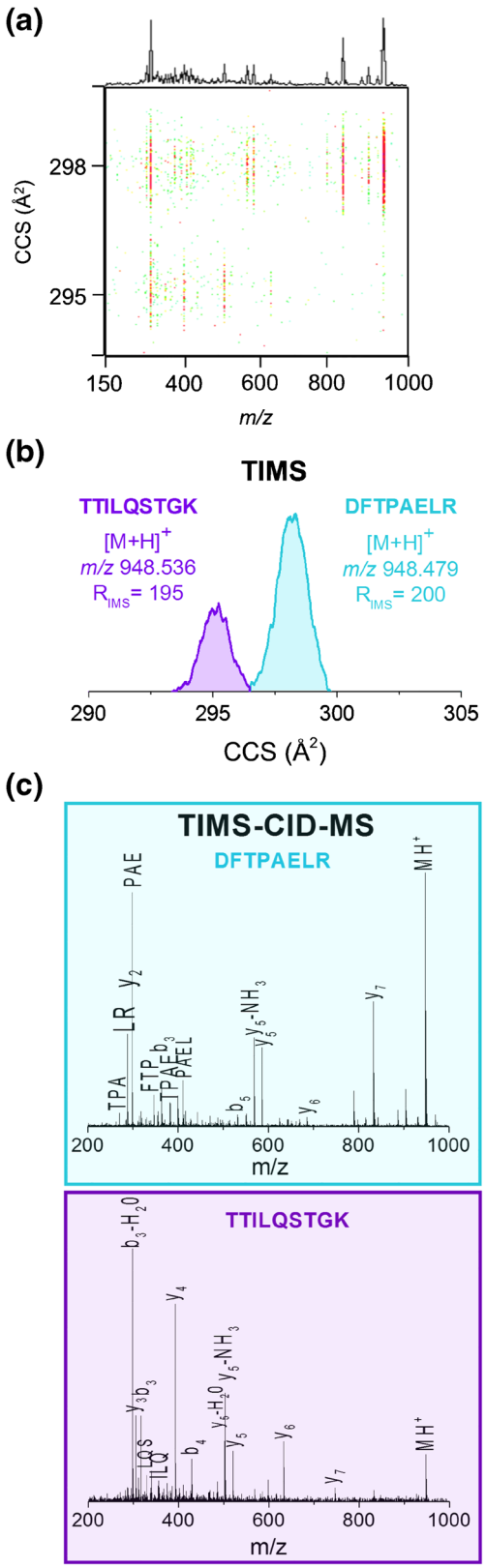

Figure 2. **(a)** TIMS-CID-TOF MS of isolated isobaric precursor ions for the DFTPAELR and TTILQSTGK peptides and the corresponding ladder fragmentation pattern. **(b)** Mobility selected MS showing the separation of the precursor ions. **(c)** CID spectra of the fragments corresponding to DFTPAELR and TTILQSTGK

Despite the LC pre-fractionation step, the samples of interest provided highly complex spectra with multiple peaks present at the nominal mass level in the 2D-IMS-MS domain (Figure 3a). The 2D IMS-MS contour plots showed that each fraction contained two main trend lines, corresponding to singly and doubly charged species [8]. Closer inspection confirmed that the TTILQSTGK $[M+H]^+$ molecular ion (*m/z* 948.536) was accompanied by two other compounds within 5 mDa, which are not distinctly separated in the MS domain alone, despite the high mass resolution of the TOF analyzer (R_{MS} ~30–40 k). When combined with TIMS analysis, however, the three signals can be easily separated, distinguished, and identified (Figure 3b). Further comparison of the targeted peptide and the corresponding heavy analog IMS projections of TTILQSTGK $[M+H]^+$ (*m/z* 956.555) confirmed the assignment in the 2D-IMS-MS contour plots (Figure 3c).

After verifying the TIMS-MS workflow for high reproducibility and accuracy in measuring and identifying the targeted peptides from the WHIM16 tryptic digested fractions, the potential for quantitative analysis via TIMS-MS was evaluated. To mimic matrix effects, one of the fractions with confirmed absence of the target peptide was spiked with known concentrations of the light and heavy peptide standards. The use of internal heavy standards accounted for variations in the nanoESI spray between experiments and from sample to sample, as well as changes in the spraying conditions as a function of time. Figure 4 shows a linear dependence between the TIMS peak area and the sample concentration for the case of the TTILQSTGK $[M+H]^+$ peptide (Figure 4a), regardless of the TIMS trapping time (e.g., t_{ramp} = 100–500 ms) and analytical ramp slope (Figure 4b). The robustness of this TIMS-MS quantitation procedure was also confirmed for all the peptides of interest at the low concentration (e.g., 1, 5, 10, and 20 nM) and the use of internal heavy peptide analogs accounted for all the potential nanoESI spray variability (Figure 4c).

The analysis and quantitation of targeted compounds in complex mixtures using direct infusion ESI (and nanoESI) can be subject to ion suppression effects [66, 67]. To further evaluate this consequence, dilution (up to 20 times) of a WHIM16 tryptic digested fraction with known spiked concentrations of targeted and heavy standards showed less than 10% variability in the TIMS-MS quantification results (Figure 5a, top). Complementary LC-ESI-MS/MS based traditional

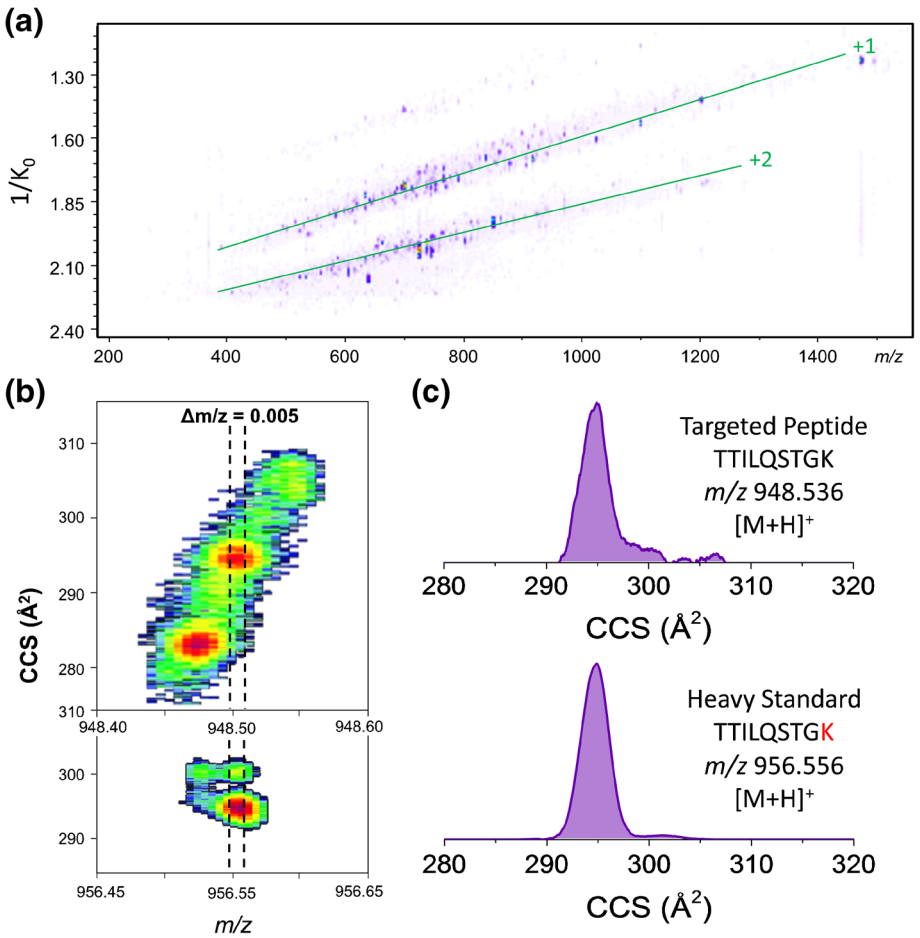

Figure 3. **(a)** Typical 2D-IMS-MS contour plot using nanoESI-TIMS-TOF MS for a fraction containing the target peptide TTILQSTGK. The 2D-IMS-MS profile highlights the complexity of each fraction and shows the charge state specific trend lines. **(b)** The 2D IMS-MS at the level of nominal mass depicts the isomeric interferences in the region of the targeted peptide and heavy analog. **(c)** IMS projection plots for the targeted and corresponding heavy peptide using 5 mDa window show identical IMS profiles

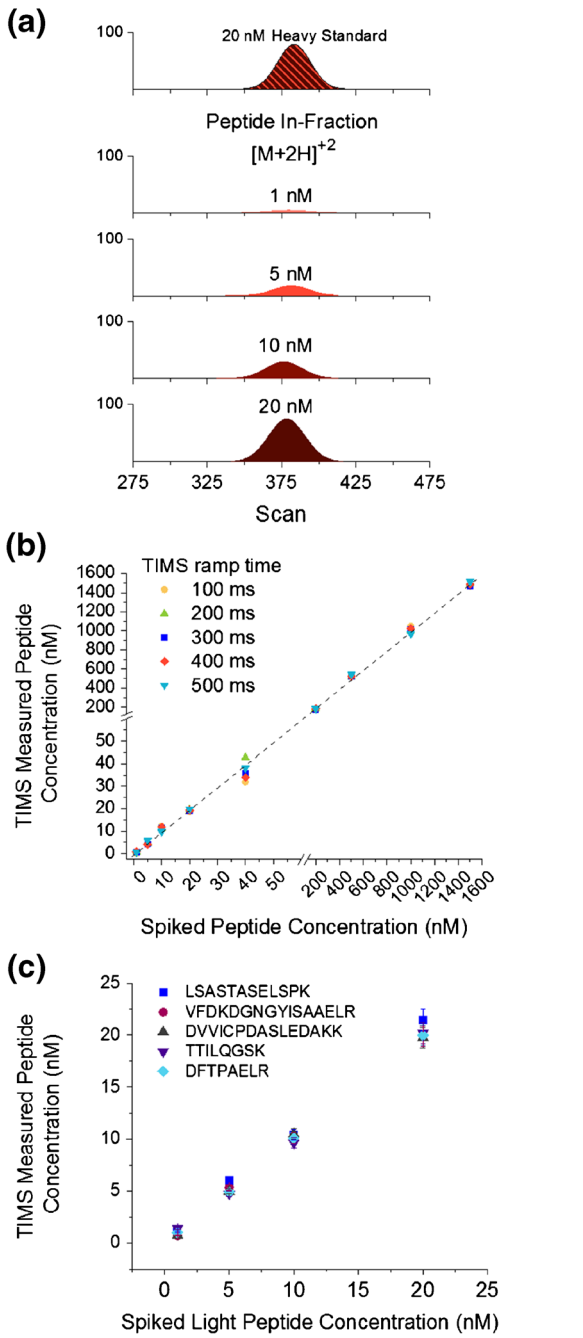

Figure 4. **(a)** Typical IMS profiles of a pure heavy standard and in-fraction light peptide standard (TTILQSTGK $[M+H]^+$) as a function of the concentration. **(b)** Trapping efficiency of TIMS-TOF MS analysis illustrating that trapping time does not impact the calculated concentration or linear response. **(c)** Measured light peptide concentrations for each targeted peptide, via TIMS-TOF MS, in relation to the heavy analog displaying a linear response

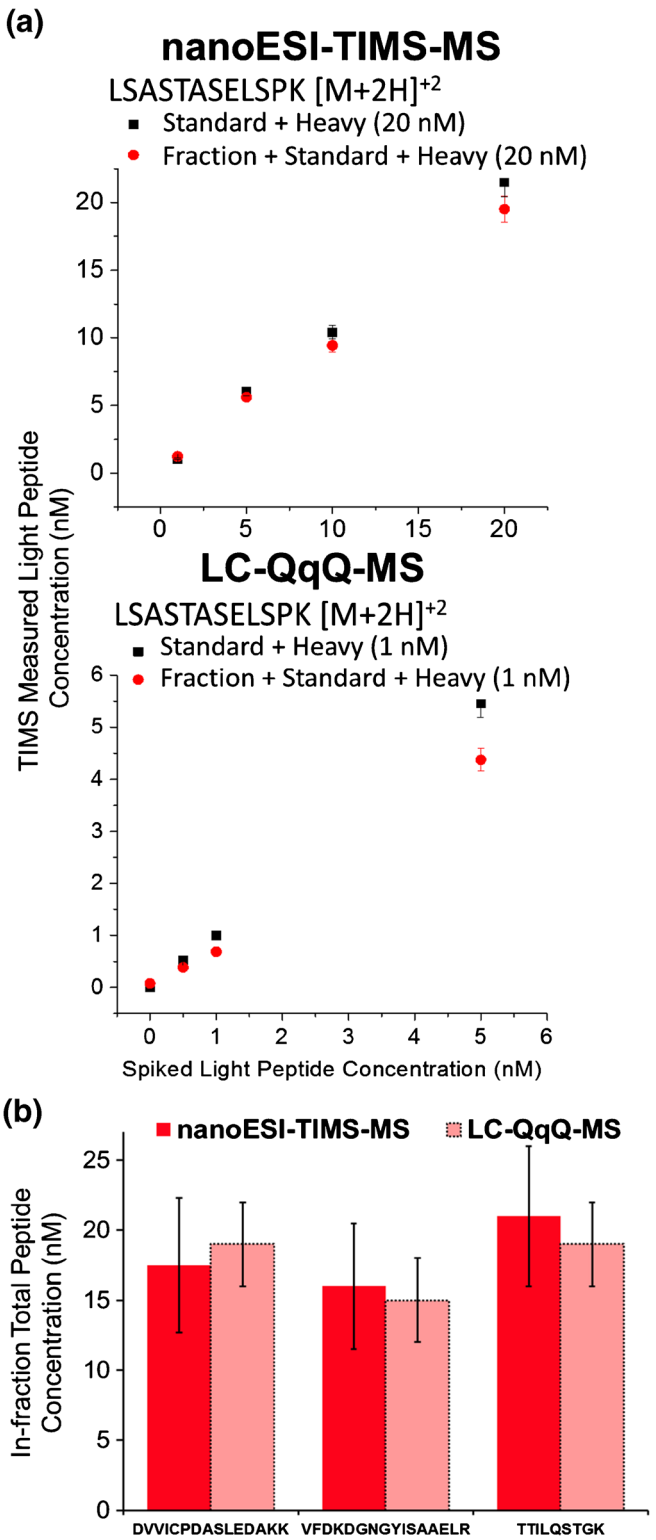

Figure 5. **(a)** Response curves for the LSASTASELSPK $[M+2H]^{+2}$ peptide standards analyzed in fraction (matrix effect) and in the blank via nanoESI-TIMS-TOF MS and LC-QqQ-MS. **(b)** Comparisons of targeted peptide concentrations measured in fractions by nanoESI-TIMS-TOF MS and LC-ESI-MS/MS

proteomic analyses of the same sample showed similar ion suppression effects (Figure 5a, bottom).

The ultimate test for the TIMS-MS workflow consisted of blind analysis of WHIM16 tryptic digested fractions known to have the targeted peptides. Briefly, the highest concentration of the targeted peptide observed was for DFTPAELR at 182 ± 7.0 nM (364 fmol/µg), followed by TTILQSTGK peptide at 21.0 ±

5.0 nM (42 fmol/μg), VFDKDGNGYISAAELR peptide at 16.0 ± 4.5 nM (32 fmol/μg), DVVICPDASLEDAKK peptide at 18 ± 5.0 nM (35 fmol/μg), and LSASTASELSPK peptide at 17 ± 4.8 nM (33 fmol/μg). The results of the TIMS-MS quantification procedure and their comparison to LC-ESI-MS/MS-based traditional proteomic analyses of the same sample are summarized in Figure 5b and Table 1. Overall, comparable results for targeted peptides per fraction were observed using nanoESI-TIMS-MS and LC-ESI-MS/MS; moreover, it is worth stating that while nanoESI-TIMS-MS was routinely done in 5 min, each LC-ESI-MS/MS analysis typically required 20–25 min. In addition, while TIMS-MS measurements were geared toward the separation, identification, and quantitation of five targeted peptides, simultaneously, discovery TIMS-MS measurements were collected without compromising the targeted analysis. That is, the TIMS-MS analysis allowed for the identification of multiple tryptic peptides (both targeted and untargeted) from the above five specified proteins. For example, TIMS-MS data analysis revealed 15% to 60% protein sequence coverage, using peptide IDs that were not initially targeted, over the various fractions analyzed (see Supplementary Figure S1 and Supplementary Table S1 in the Supporting Information). While new biomarker detection is not in the scope of the present study, it should be noted that a posteriori screening (or discovery) of potential biomarkers of interest is an inherent potential of the current TIMS-MS workflow. That is, the use of TIMS-MS workflow as a broad measurement technique, concurrently with the targeted quantitative approach, effectively reduces the problems associated with individual analyses and holds the advantage of increasing proteome coverage and new biomarker detection while maintaining speed, accuracy and sensitivity.

Conclusions

The demand for fast, accurate, and sensitive analytical tools for the detection and quantification of biomolecules is increasing as a way to offset the challenge of drug discovery and biomarker identification. While several strategies have been developed, some current efforts are focused on reducing sample preparation and analysis time, while increasing detection limits and peak capacity by using complementary, orthogonal separation techniques. In the present work, the concepts of characterizing proteomes using offline nanoESI-TIMS-MS were evaluated by performing targeted and discovery analysis of cancer biomarkers from a human-in-mouse xenograft tumor tissue. Results showed that targeted peptide separation, identification, and sequencing can be performed based on accurate CCS, *m/z*, and fragmentation pattern measurements, and that peptide quantitation can be routinely achieved utilizing heavy peptide analogs as internal standards. The capacity of the TIMS analyzer for selective mobility trapping with high resolving power increases the selectivity and sensitivity of the analysis and provides unique advantages for offline targeted studies compared with traditional LC-ESI-MS-MS proteomic strategies. A good agreement was obtained between the quantitation using offline nanoESI-TIMS-MS and LC-ESI-MS/MS. This work serves as a stepping stone and proof of concept for quantitative proteomics of targeted peptides without the need for online LC separation, an aspect that can significantly lower the analysis cost and lead to increased sample throughput during targeted biomarker detection.

Acknowledgements

This work was supported by the National Cancer Institute (NCI) through Leidos Biomedical Inc. (no. 14X2333 to FFL) and National Institute of General Medicine (Grant no. R00GM106414 to FFL). The PNNL efforts were performed in the Environmental Molecular Sciences Laboratory, a US Department of Energy (DOE) national scientific user facility located at PNNL in Richland, WA. The authors acknowledge the support from Kristin E. Burnum-Johnson and Marina A. Gritsenko for the liquid chromatography fractionation and peptide selection per fraction. PNNL is a multi-program national laboratory operated by Battelle Memorial Institute for the DOE under Contract DE-AC05-76RL01830.

References

1. King, R., Bonfiglio, R., Fernandez-Metzler, C., Miller-Stein, C., Olah, T.: Mechanistic investigation of ionization suppression in electrospray ionization. J. Am. Soc. Mass Spectrom. **11**, 942–950 (2000)
2. Lin, L., Yu, Q., Yan, X., Hang, W., Zheng, J., Xing, J., Huang, B.: Direct infusion mass spectrometry or liquid chromatography mass spectrometry for human metabonomics? A serum metabonomic study of kidney cancer. Analyst. **135**, 2970–2978 (2010)
3. Aebersold, R., Mann, M.: Mass-spectrometric exploration of proteome structure and function. Nature. **537**, 347–355 (2016)
4. Grebe, S.K.G., Singh, R.J.: LC-MS/MS in the Clinical Laboratory – Where to from here? Clin. Biochem. Rev. **32**, 5–31 (2011)
5. Holland, J.F., Enke, C.G., Allison, J., Stults, J.T., Pinkston, J.D., Newcome, B., Watson, J.T.: Mass spectrometry on the chromatographic time scale: realistic expectations. Anal. Chem. **55**, 997A–1012A (1983)
6. Valentine, S.J., Counterman, A.E., Hoaglund, C.S., Reilly, J.P., Clemmer, D.E.: Gas-phase separations of protease digests. J. Am. Soc. Mass Spectrom. **9**, 1213–1216 (1998)
7. Bohnenberger, H., Ströbel, P., Mohr, S., Corso, J., Berg, T., Urlaub, H., Lenz, C., Serve, H., Oellerich, T.: Quantitative mass spectrometric profiling of cancer-cell proteomes derived from liquid and solid tumors. JOVE-J. Vis. Exp. (2015)
8. Meier, F., Beck, S., Grassl, N., Lubeck, M., Park, M.A., Raether, O., Mann, M.: Parallel accumulation-serial fragmentation (PASEF): multiplying sequencing speed and sensitivity by synchronized scans in a trapped ion mobility device. J. Proteome Res. **14**, 5378–5387 (2015)
9. Lanucara, F., Holman, S.W., Gray, C.J., Eyers, C.E.: The power of ion mobility-mass spectrometry for structural characterization and the study of conformational dynamics. Nat. Chem. **6**, 281–294 (2014)
10. Benigni, P., Thompson, C.J., Ridgeway, M.E., Park, M.A., Fernandez-Lima, F.A.: Targeted high-resolution ion mobility separation coupled to ultrahigh-resolution mass spectrometry of endocrine disruptors in complex mixtures. Anal. Chem. **87**, 4321–4325 (2015)
11. Valentine, S.J., Plasencia, M.D., Liu, X., Krishnan, M., Naylor, S., Udseth, H.R., Smith, R.D., Clemmer, D.E.: Toward plasma proteome profiling with ion mobility-mass spectrometry. J. Proteome Res. **5**, 2977–2984 (2006)
12. Venne, K., Bonneil, E., Eng, K., Thibault, P.: Improvement in peptide detection for proteomics analyses using nanoLC-MS and high-field

asymmetry waveform ion mobility mass spectrometry. Anal. Chem. **77**, 2176–2186 (2005)
13. Shliaha, P.V., Bond, N.J., Gatto, L., Lilley, K.S.: Effects of traveling wave ion mobility separation on data independent acquisition in proteomics studies. J. Proteome Res. **12**, 2323–2339 (2013)
14. Srebalus Barnes, C.A., Hilderbrand, A.E., Valentine, S.J., Clemmer, D.E.: Resolving isomeric peptide mixtures: a combined HPLC/ion mobility-TOFMS analysis of a 4000-component combinatorial library. Anal. Chem. **74**, 26–36 (2002)
15. Bohrer, B.C., Merenbloom, S.I., Koeniger, S.L., Hilderbrand, A.E., Clemmer, D.E.: Biomolecule analysis by ion mobility spectrometry. Annu. Rev. Anal. Chem. **1**, 293–327 (2008)
16. Merenbloom, S.I., Bohrer, B.C., Koeniger, S.L., Clemmer, D.E.: Assessing the peak capacity of IMS-IMS separations of tryptic peptide ions in He at 300 K. Anal. Chem. **79**, 515–522 (2007)
17. Liu, X., Valentine, S.J., Plasencia, M.D., Trimpin, S., Naylor, S., Clemmer, D.E.: Mapping the human plasma proteome by SCX-LC-IMS-MS. J. Am. Soc. Mass Spectrom. **18**, 1249–1264 (2007)
18. McLean, J.A., Ruotolo, B.T., Gillig, K.J., Russell, D.H.: Ion mobility-mass spectrometry: a new paradigm for proteomics. Int. J. Mass Spectrom. **240**, 301–315 (2005)
19. Zinnel, N.F., Pai, P.-J., Russell, D.H.: Ion mobility-mass spectrometry (IM-MS) for top-down proteomics: increased dynamic range affords increased sequence coverage. Anal. Chem. **84**, 3390–3397 (2012)
20. Fernandez-Lima, F.A., Kaplan, D.A., Suetering, J., Park, M.A.: Gas-phase separation using a trapped ion mobility spectrometer. Int. J. Ion Mobil. Spectrom. **14**, 93–98 (2011)
21. Fernandez-Lima, F.A., Kaplan, D.A., Park, M.A.: Note: integration of trapped ion mobility spectrometry with mass spectrometry. Rev. Sci. Instrum. **82**, 126106 (2011)
22. Castellanos, A., Benigni, P., Hernandez, D.R., DeBord, J.D., Ridgeway, M.E., Park, M.A., Fernandez-Lima, F.A.: Fast screening of polycyclic aromatic hydrocarbons using trapped ion mobility spectrometry-mass spectrometry. Anal. Methods. **6**, 9328–9332 (2014)
23. Schenk, E.R., Mendez, V., Landrum, J.T., Ridgeway, M.E., Park, M.A., Fernandez-Lima, F.: Direct observation of differences of carotenoid polyene chain cis/trans isomers resulting from structural topology. Anal. Chem. **86**, 2019–2024 (2014)
24. Molano-Arevalo, J.C., Hernandez, D.R., Gonzalez, W.G., Miksovska, J., Ridgeway, M.E., Park, M.A., Fernandez-Lima, F.: Flavin adenine dinucleotide structural motifs: from solution to gas phase. Anal. Chem. **86**, 10223–10230 (2014)
25. Schenk, E.R., Ridgeway, M.E., Park, M.A., Leng, F., Fernandez-Lima, F.: Isomerization kinetics of AT hook decapeptide solution structures. Anal. Chem. **86**, 1210–1214 (2014)
26. McKenzie, A., DeBord, J.D., Ridgeway, M.E., Park, M.A., Eiceman, G.A., Fernandez-Lima, F.: Lifetimes and stabilities of familiar explosives molecular adduct complexes during ion mobility measurements. Analyst. **140**, 5692–5699 (2015)
27. Hernandez, D.R., DeBord, J.D., Ridgeway, M.E., Kaplan, D.A., Park, M.A., Fernandez-Lima, F.A.: Ion dynamics in a trapped ion mobility spectrometer. Analyst. **139**, 1913–1921 (2014)
28. Schenk, E.R., Nau, F., Fernandez-Lima, F.: Theoretical predictor for candidate structure assignment from IMS data of biomolecule-related conformational space. Int. J. Ion Mobil. Spectrom. **18**, 23–29 (2015)
29. Schenk, E.R., Almeida, R., Miksovska, J., Ridgeway, M.E., Park, M.A., Fernandez-Lima, F.: Kinetic Intermediates of Holo- and Apo-myoglobin studied using HDX-TIMS-MS and molecular dynamic simulations. J. Am. Soc. Mass Spectrom. **26**, 555–563 (2015)
30. Adams, K.J., Montero, D., Aga, D., Fernandez-Lima, F.: Isomer separation of polybrominated diphenyl ether metabolites using nanoESI-TIMS-MS. Int. J. Ion Mobil. Spectrom. **19**, 69–76 (2016)
31. Benigni, P., Fernandez-Lima, F.: Oversampling selective accumulation trapped ion mobility spectrometry coupled to FT-ICR MS: fundamentals and applications. Anal. Chem. **88**, 7404–7412 (2016)
32. Benigni, P., Marin, R., Molano-Arevalo, J.C., Garabedian, A., Wolff, J.J., Ridgeway, M.E., Park, M.A., Fernandez-Lima, F.: Towards the analysis of high molecular weight proteins and protein complexes using TIMS-MS. Int. J. Ion Mobil. Spectrom. **19**, 95–104 (2016)
33. Garabedian, A., Butcher, D., Lippens, J.L., Miksovska, J., Chapagain, P.P., Fabris, D., Ridgeway, M.E., Park, M.A., Fernandez-Lima, F.: Structures of the kinetically trapped i-motif DNA intermediates. Phys. Chem., Chem. Phys. **18**, 26691–26702 (2016)
34. Zeleny, J.: On the ratio of velocities of the two ions produced in gases by Röngten radiation, and on some related phenomena. Philos. Mag. **46**, 120–154 (1898)
35. Benigni, P., Sandoval, K., Thompson, C.J., Ridgeway, M.E., Park, M.A., Gardinali, P., Fernandez-Lima, F.: Analysis of photoirradiated water accommodated fractions of crude oils using tandem TIMS and FT-ICR MS. Environ. Sci. Technol. **51**, 5978–5988 (2017)
36. Silveira, J.A., Ridgeway, M.E., Laukien, F.H., Mann, M., Park, M.A.: Parallel accumulation for 100% duty cycle trapped ion mobility-mass spectrometry. Int. J. Mass Spectrom. **413**, 168–175 (2017)
37. Michelmann, K., Silveira, J.A., Ridgeway, M.E., Park, M.A.: Fundamentals of trapped ion mobility spectrometry. J. Am. Soc. Mass Spectrom. **26**, 14–24 (2015)
38. Silveira, J.A., Michelmann, K., Ridgeway, M.E., Park, M.A.: Fundamentals of trapped ion mobility spectrometry. Part II: fluid dynamics. J. Am. Soc. Mass Spectrom. **27**, 585–595 (2016)
39. Silveira, J.A., Danielson, W., Ridgeway, M.E., Park, M.A.: Altering the mobility-time continuum: nonlinear scan functions for targeted high resolution trapped ion mobility-mass spectrometry. Int. J. Ion Mobil. Spectrom. **19**, 87–94 (2016)
40. Ridgeway, M.E., Silveira, J.A., Meier, J.E., Park, M.A.: Microheterogeneity within conformational states of ubiquitin revealed by high resolution trapped ion mobility spectrometry. Analyst. **140**, 6964–6972 (2015)
41. Silveira, J.A., Ridgeway, M.E., Park, M.A.: High resolution trapped ion mobility spectrometery of peptides. Anal. Chem. **86**, 5624–5627 (2014)
42. Ridgeway, M.E., Wolff, J.J., Silveira, J.A., Lin, C., Costello, C.E., Park, M.A.: Gated trapped ion mobility spectrometry coupled to fourier transform ion cyclotron resonance mass spectrometry. Int. J. Ion Mobil. Spectrom. **19**, 77–85 (2016)
43. Pu, Y., Ridgeway, M.E., Glaskin, R.S., Park, M.A., Costello, C.E., Lin, C.: Separation and identification of isomeric glycans by selected accumulation-trapped ion mobility spectrometry-electron activated dissociation tandem mass spectrometry. Anal. Chem. **88**, 3440–3443 (2016)
44. Liu, F.C., Kirk, S.R., Bleiholder, C.: On the structural denaturation of biological analytes in trapped ion mobility spectrometry-mass spectrometry. Analyst. **141**, 3722–3730 (2016)
45. Ntai, I., LeDuc, R.D., Fellers, R.T., Erdmann-Gilmore, P., Davies, S.R., Rumsey, J., Early, B.P., Thomas, P.M., Li, S., Compton, P.D., Ellis, M.J.C., Ruggles, K.V., Fenyö, D., Boja, E.S., Rodriguez, H., Townsend, R.R., Kelleher, N.L.: Integrated bottom-up and top-down proteomics of patient-derived breast tumor xenografts. Mol. Cell. Proteom. **15**, 45–56 (2016)
46. Wang, Y., Yang, F., Gritsenko, M.A., Wang, Y., Clauss, T., Liu, T., Shen, Y., Monroe, M.E., Lopez-Ferrer, D., Reno, T., Moore, R.J., Klemke, R.L., Camp, D.G., Smith, R.D.: Reversed-phase chromatography with multiple fraction concatenation strategy for proteome profiling of human MCF10A cells. Proteomics. **11**, 2019–2026 (2011)
47. McDaniel, E.W., Mason, E.A.: John Wiley and Sons, Inc., New York, NY (1973)
48. Ismail, I.A., Kang, H.S., Lee, H.J., Kim, J.K., Hong, S.H.: DJ-1 upregulates breast cancer cell invasion by repressing KLF17 expression. Br. J. Cancer. **110**, 1298–1306 (2014)
49. Li, Z., Joyal, J.L., Sacks, D.B.: Calmodulin enhances the stability of the estrogen receptor. J. Biol. Chem. **276**, 17354–17360 (2001)
50. Rozenblatt-Rosen, O., Hughes, C.M., Nannepaga, S.J., Shanmugam, K.S., Copeland, T.D., Guszczynski, T., Resau, J.H., Meyerson, M.: The parafibromin tumor suppressor protein is part of a human Paf1 complex. Mol. Cell. Biol. **25**, 612–620 (2005)
51. Selvarajan, S., Sii, L.H., Lee, A., Yip, G., Bay, B.H., Tan, M.H., Teh, B.T., Tan, P.H.: Parafibromin expression in breast cancer: a novel marker for prognostication? J. Clin. Pathol. **61**, 64–67 (2008)
52. Jordan, M.A., Wilson, L.: Microtubules as a target for anticancer drugs. Nat. Rev. Cancer. **4**, 253–265 (2004)
53. Cassimeris, L., Spittle, C.: Regulation of microtubule-associated proteins. Int. Rev. Cytol. **210**, 163–226 (2001)
54. Bhat, K.M.R., Setaluri, V.: Microtubule-associated proteins as targets in cancer chemotherapy. Clin. Cancer Res. **13**, 2849–2854 (2007)
55. Ahmed, I.S., Rohe, H.J., Twist, K.E., Mattingly, M.N., Craven, R.J.: Progesterone receptor membrane component 1 (PGRMC1): a Heme-1 domain protein that promotes tumorigenesis and is inhibited by a small molecule. J. Pharm. Exp. Ther. **333**, 564–573 (2010)
56. Xu, J., Zeng, C., Chu, W., Pan, F., Rothfuss, J.M., Zhang, F., Tu, Z., Zhou, D., Zeng, D., Vangveravong, S., Johnston, F., Spitzer, D., Chang, K.C., Hotchkiss, R.S., Hawkins, W.G., Wheeler, K.T., Mach, R.H.:

Identification of the PGRMC1 protein complex as the putative sigma-2 receptor binding site. Nat. Commun. **2**, 380 (2011)
57. Burnum-Johnson, K.E., Nie, S., Casey, C.P., Monroe, M.E., Orton, D.J., Ibrahim, Y.M., Gritsenko, M.A., Clauss, T.R.W., Shukla, A.K., Moore, R.J., Purvine, S.O., Shi, T., Qian, W., Liu, T., Baker, E.S., Smith, R.D.: Simultaneous proteomic discovery and targeted monitoring using liquid chromatography, ion mobility spectrometry and mass spectrometry. Mol. Cell. Proteom. **15**, 3694–3705 (2016)
58. May, J.C., Goodwin, C.R., Lareau, N.M., Leaptrot, K.L., Morris, C.B., Kurulugama, R.T., Mordehai, A., Klein, C., Barry, W., Darland, E., Overney, G., Imatani, K., Stafford, G.C., Fjeldsted, J.C., McLean, J.A.: Conformational ordering of biomolecules in the gas phase: nitrogen collision cross sections measured on a prototype high resolution drift tube ion mobility-mass spectrometer. Anal. Chem. **86**, 2107–2116 (2014)
59. Merenbloom, S.L., Koeniger, S.L., Bohrer, B.C., Valentine, S.J., Clemmer, D.E.: Improving the efficiency of IMS-IMS by a combing technique. Anal. Chem. **80**, 1918–1927 (2008)
60. Fernandez-Lima, F.A., Becker, C., Gillig, K.J., Russell, W.K., Tichy, S.E., Russell, D.H.: Ion mobility-mass spectrometer interface for collisional activation of mobility separated ions. Anal. Chem. **81**, 618–624 (2009)
61. Stone, E.G., Gillig, K.J., Ruotolo, B.T., Russell, D.H.: Optimization of a matrix-assisted laser desorption ionization-ion mobility-surface-induced dissociation-orthogonal-time-of-flight mass spectrometer: simultaneous acquisition of multiple correlated MS1 and MS2 spectra. Int. J. Mass Spectrom. **212**, 519–533 (2001)
62. Pringle, S.D., Giles, K., Wildgoose, J.L., Williams, J.P., Slade, S.E., Thalassinos, K., Bateman, R.H., Bowers, M.T., Scrivens, J.H.: An investigation of the mobility separation of some peptide and protein ions using a new hybrid quadrupole/traveling wave IMS/oa-ToF instrument. Int. J. Mass Spectrom. **261**, 1–12 (2007)
63. Baker, E.S., Tang, K., Danielson, W.F., Prior, D.C., Smith, R.D.: Simultaneous fragmentation of multiple ions using IMS drift time dependent collision energies. J. Am. Soc. Mass Spectrom. **19**, 411–419 (2008)
64. Valentine, S.J., Koeniger, S.L., Clemmer, D.E.: A split-field drift tube for separation and efficient fragmentation of biomolecular ions. Anal. Chem. **75**, 6202–6208 (2003)
65. Lee, Y.J., Hoaglund-Hyzer, C.S., Taraszka, J.A., Zientara, G.A., Counterman, A.E., Clemmer, D.E.: Collision-induced dissociation of mobility-separated ions using an orifice-skimmer cone at the back of a drift tube. Anal. Chem. **73**, 3549–3555 (2001)
66. Taylor, P.J.: Matrix effects: the Achilles heel of quantitative high-performance liquid chromatography-electrospray-tandem mass spectrometry. Clin. Biochem. **38**, 328–334 (2005)
67. Cappiello, A., Famiglini, G., Palma, P., Pierini, E., Termopoli, V., Trufelli, H.: Overcoming matrix effects in liquid chromatography-mass spectrometry. Anal. Chem. **80**, 9343–9348 (2008)